

Retrospective Gating for Mouse Cardiac MRI

Jonathan Bishop,^{1*} Akiva Feintuch,¹ Nicholas A. Bock,^{1,2} Brian Nieman,^{1,2} Jun Dazai,¹ Lorinda Davidson,¹ and R. Mark Henkelman^{1,2}

Cardiac MR imaging in small animals presents some difficulties due to shorter cardiac cycles and smaller dimensions than in human beings, but prospectively gated techniques have been successfully applied. As with human imaging, there may be certain applications in animal imaging for which retrospective gating is preferable to prospective gating. For example, cardiac imaging in multiple mice simultaneously is one such application. In this work we investigate the use of retrospective gating for cardiac imaging in a mouse. Using a three-dimensional imaging protocol, we show that image quality with retrospective gating is comparable to prospectively gated imaging. We conclude that retrospective gating is applicable for small animal cardiac MRI and show how it can be applied to the problem of cardiac MRI in multiple mice. Magn Reson Med 55:472–477, 2006. © 2006 Wiley-Liss, Inc.

Key words: retrospective; cardiac; gating; multiple mouse; cine

In recent years, many new animal models have been developed to study human cardiac development and disease processes. The mouse has been identified as a particularly useful animal model due to its genetic similarity with humans, the availability of powerful genetic techniques, and relatively low cost of production and maintenance (1,2). As a result, many different imaging techniques are being developed to analyze these various mouse models for anatomic and functional phenotypes, as well as to screen random mutants for new models of human disease. In particular, MR imaging for mouse models of human cardiac disease has shown great promise. The challenges of small animal MR imaging compared to conventional human imaging include faster heart rates and no option for breath holding. Despite these difficulties, very good results have been obtained (3,4) by employing the techniques of human cardiac imaging. These prior studies have employed prospective gating for the purposes of resolving the cardiac motion and eliminating respiratory motion.

In cardiac imaging of the mouse, scan time and throughput are important issues because signal/noise ratio scales poorly with decreased animal size and, thus, scan times are considerably longer for mouse imaging compared to human imaging. Furthermore, large numbers of mice may be required to investigate specific biologic questions. Im-

aging of several mice in parallel is a new technique that has been introduced to address high-throughput imaging of mice (5). This technique employs separate, well-isolated coils and receivers per mouse in conjunction with a common gradient coil in order to obtain MR images of separate mice in parallel. While excellent results have been obtained for in vivo brain (6) and for fixed whole body (7), it has not yet been shown that cardiac imaging can be performed on multiple mice in parallel; there is no way to implement any form of prospective gating, since the cardiac motion of the various animals is completely asynchronous.

The goal of this work is to establish the feasibility of cardiac imaging of multiple mice by solving the gating problem. We propose to use retrospective gating as the main strategy for imaging multiple mice. Although retrospective gating is less efficient and offers less motion control than prospective techniques, it has previously been applied in animal computed tomography (CT) (8,9) and it is well-suited to the problem of cardiac imaging in several mice because it reduces the gating problem to one of recording the physiologic waveforms of the multiple live mice in parallel. If parallel monitoring can be arranged, then the cardiac motion may as easily be reconstructed for an arbitrary number of mice as for one. The scope of this article is therefore to compare retrospective gating with prospective gating in a single mouse and to demonstrate retrospectively gated cardiac images obtained in several mice in parallel.

MATERIALS AND METHODS

Combined cardiac and respiratory retrospective gating has been described previously for human imaging (10,11). Briefly, the pulse sequence runs continuously, and as a result is asynchronous to the physiologic waveforms. The ECG and respiration are recorded over the length of the entire scan. In human imaging, respiratory gating can be derived from navigator echoes (3); but if one assumes that live mouse imaging is severely SNR-limited, then the scan time overhead associated with navigator echoes may be undesirable and the respiratory information can be collected with a bellows or other similar device. At the completion of the scan, each *k*-space frame is assigned a cardiac and respiratory phase based on the recorded waveforms. *K*-space data are then sorted and interpolated from the sampled time points to the time points of the desired cardiac reconstruction frames (12).

All animal utilization protocols were approved by the Hospital for Sick Children Animal Care Committee, subject to the Canadian Council on Animal Care. Mouse handling and imaging were performed as follows. The mice were anesthetized following induction with 2.0% isoflurane gas, and maintained with 1.6% gas. They were

¹Mouse Imaging Centre, Hospital for Sick Children, Toronto, Ontario, Canada.

²Department of Medical Biophysics, University of Toronto, Ontario, Canada. Grant Sponsors: Canada Foundation for Innovation, the Ontario Research and Development Challenge Fund, the National Institutes of Health, the Canada Research Chairs Program, the National Sciences and Engineering Research Council, and the National Cancer Institute of Canada.

*Correspondence to: Jonathan Bishop, Mouse Imaging Centre, Hospital for Sick Children, 555 University Avenue, Toronto, ON, M5G 1X8, Canada. E-mail: jbishop@phenogenomics.ca

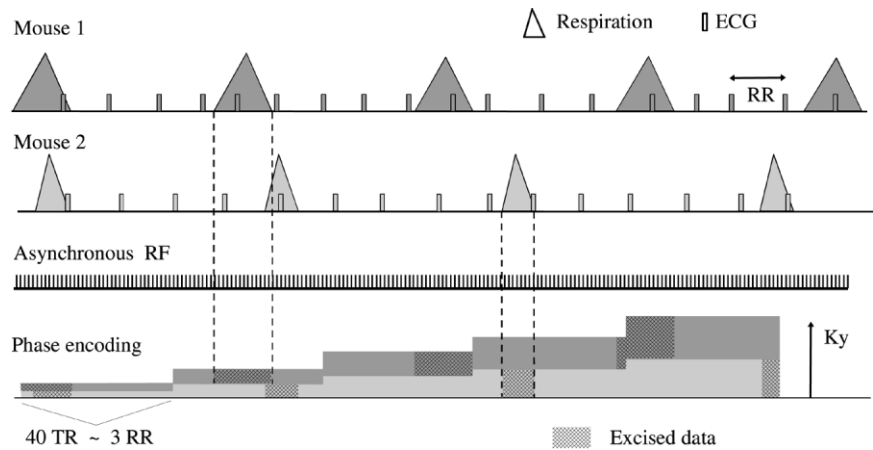
Received 15 November 2004; revised 20 October 2005; accepted 1 November 2005.

DOI 10.1002/mrm.20794

Published online 31 January 2006 in Wiley InterScience (www.interscience.wiley.com).

© 2006 Wiley-Liss, Inc.

FIG. 1. Cardiac and respiratory diagram for multiple mouse MRI. Physiologic waveforms are indicated for 2 mice, both running asynchronously to the pulse sequence. The k -space phase encoding is empirically assigned to increment every 3–6 RR intervals. This ensures that sufficient k -space acquisitions have been made to sample each RR and respiration interval while allowing for natural variation over the scan. During reconstruction, any k -space frame corrupted by the respiration of one mouse is thrown out for that mouse but retained for the others.



loaded on a custom built sled (6) with built-in physiologic monitoring apparatus. ECG electrodes were fastened to the shaved chest with conductive hydrogel, while respiration was monitored with a pneumatic pillow. ECG and respiration were monitored using commercial hardware (Small Animal Instruments Inc., Stonybrook, NY, USA) and recorded on a four-channel oscilloscope along with time stamp pulses from the scanner. Three-dimensional spoiled gradient-echo imaging was performed with a 7T MRI scanner (Varian INOVA, Palo Alto, CA, USA). Two imaging protocols were used. Single mouse scans for purposes of comparing retrospective to prospective gating were acquired with $TR/TE = 10/1.8$ ms. The short-axis slab was encoded with a matrix of $160 \times 160 \times 16$ and voxel size of $150 \times 150 \times 750 \mu\text{m}^3$. A 6 cm inner diameter gradient coil (Magnex 115/60, 1000 mT/m maximum amplitude, 150 μs rise time) was used for single mouse scans. Each ky - kz phase encoding step was sampled 60 times (about 5 RR intervals) to resolve both the cardiac cycle and respiratory motion. Total scan time was about 25 min. The multiple mouse protocol was acquired with $TR/TE = 70/4.5$ ms and black blood preparation (13), using a 29 cm bore gradient coil (Tesla, 120 mT/m maximum amplitude, 867 μs rise time). Short-axis slabs were encoded with a matrix of $120 \times 120 \times 8$ and voxel size of $200 \times 200 \times 750 \mu\text{m}^3$. Each ky - kz phase encoding step was sampled 50 times and resolved only the cardiac cycle. Total scan time was about 60 min.

The basic task of sorting and discarding motion-corrupted data can be seen in Fig. 1. In this figure, the cardiac and respiratory waveforms for two mice are shown schematically, in addition to a trace of the tr intervals and the progression of the phase encoding gradient. For each mouse, we begin with the complete set of k -space-time data. During the respiration events of the current mouse being reconstructed, as indicated by triangles in Fig. 1, we assume that motion is likely to have corrupted the readout frames acquired within that interval and therefore discard them. In other words, the sorting and discarding process is conducted independently for each mouse imaged, according to the independent physiologic record of each mouse. During this binning process, an important decision must be made as to where to place the bin borders, since the respiration monitor may or may not reflect the true state of

motion in the thorax near the heart. If they are set conservatively, we would expect fewer motion artifacts in the images, but since more k -space data will have been discarded, there will be lower signal/noise ratio and an overall loss of imaging efficiency. If the borders are set liberally, a greater amount of the k -space data are retained and may be used for signal averaging. An alternative to this binning process is to interpolate the data to the desired points in the respiratory cycle (14).

Data acquired in a single mouse were used for evaluating reconstruction strategies. Beginning with the 60 readout frames available for each phase encoding step, 3 retrospective reconstruction strategies were defined with different degrees of discarding and/or averaging data. The purpose of this was to evaluate the trade-off between respiratory motion artifact and signal/noise ratio in the reconstructed images. The first reconstruction strategy was to pick a set of the 36 frames least affected by respiratory motion, as determined by greatest distance in time from the nearest respiration event. The average duration of a respiratory event was ~ 200 ms, which for a TR of 10 ms consists of 20 frames. The chosen frames should therefore cover most of the “quiescent” phase of the respiration, as illustrated in Fig. 1. The respiration monitor shows that the breathing pattern of an anesthetized mouse consists of short gasps separated by longer quiescent periods, so we anticipated that this sorting should provide the best overall trade-off between signal/noise ratio and motion artifact. The second strategy was a set of 36 frames unsorted with respect to the respiration monitor. The last strategy simply selected the complete set of 60 frames.

Interpolation of the respiratory-sorted k -space data from measured time points to the desired reconstruction time points in the RR interval was the same in all cases and was performed with linear interpolation between the two nearest neighbors according to the ECG monitor data. In the reconstruction strategies described above, there were sufficient data retained to provide for signal averaging. However, the signal accumulation for averaging must take place after temporal interpolation so that the temporal phases are consistent. Thus, the temporal data were pre-sorted into 3–5 subsets of 12 phases that covered the RR interval more or less equally, so that temporal interpolation errors were more or less equal within each subset.

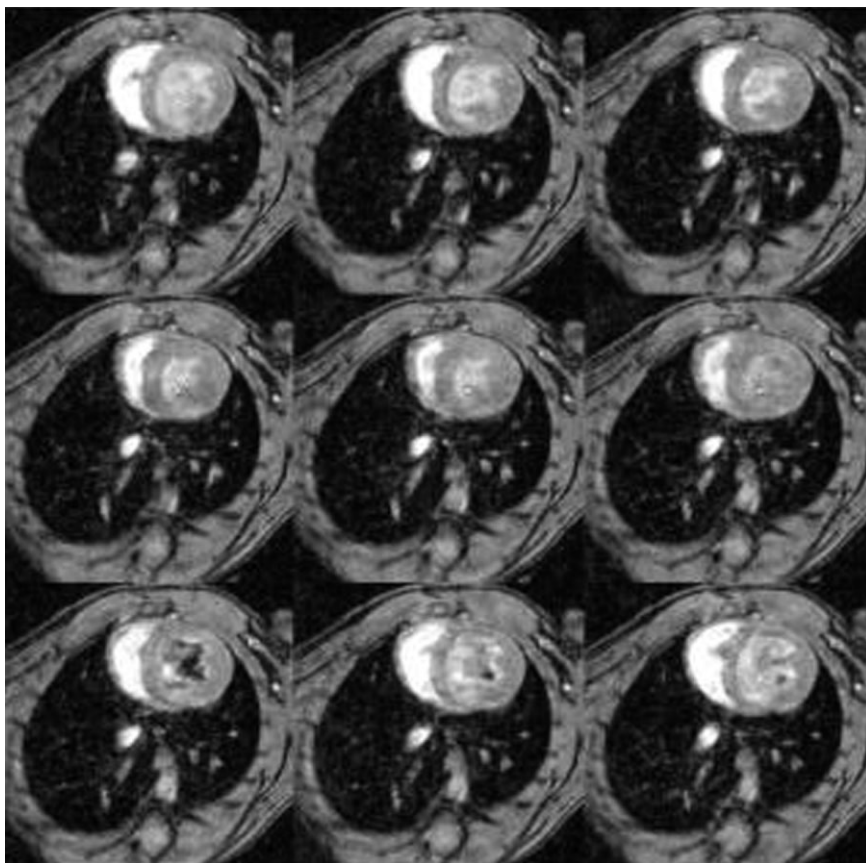


FIG. 2. A mid-axis slice reconstructed at 9 time points, with respiratory sorting. Systole begins at top left and end diastole is seen at bottom right.

Following interpolation, the subsets were then combined for simple averaging (i.e., NEX = 3–5) to improve signal/noise ratio.

Two further data sets were acquired for comparison with retrospective reconstruction. The first of these was a prospectively triggered sequence, which is the preferred technique for single mouse imaging (15–17). The sequence was double-triggered using both respiration and ECG signals, and acquired 12 readout frames per trigger event. In a final experiment, the retrospective acquisition was repeated with all room-temperature shim currents set to zero. Since individual mouse shimming of multiple mice is not feasible with a common gradient coil, this latter acquisition was made to determine whether or not shimming affected the quality of the cardiac images.

The multiple mouse scan was performed in 3 mice with cardiac-only monitoring. Since the minimum repetition time in the large-bore gradient coil was a substantial fraction of the RR interval of the anesthetized mice (150 ms), the temporal phase loop was acquired outside of the slab encode loop, to ensure the best possible random sampling of the RR interval. The combination of longer repetition time and longer echo time, relative to the single mouse scans performed with the small-bore gradient coil, resulted in both increased signal void through dephasing and increased inflow enhancement effect within different regions of the blood pool. Therefore, black-blood contrast preparation was used to null the blood signal and provide a uniform blood pool signal intensity.

RESULTS

Figure 2 shows one mid-axis slice acquired in a single mouse and reconstructed retrospectively, with respiratory sorting, at 9 temporal phases (reconstruction strategy 1 in the text above). This figure indicates that the cardiac dynamics have been captured and that a minimum of ghosting and reconstruction artifacts are seen. There is a considerable amount of dephasing in the ventricular blood pool, which is a shortcoming of the gradient echo approach with relatively long echo times (18).

Figure 3 shows one mid-axis slice acquired in a single mouse and reconstructed at 2 cardiac time points (systole and diastole). In the top row, retrospective reconstruction with respiratory sorting is shown (reconstruction strategy 1 in the text above). In the middle row, the same data set is shown with all of the data being used for simple averaging rather than respiratory sorting, thus achieving a higher signal/noise ratio (reconstruction strategy 3). Finally, the bottom row shows the prospectively gated acquisition, which has slightly higher signal intensity due to the inflow effects of the interrupted steady-state.

In the test of shimming in a single mouse, the linewidth of the cardiac slab increased from 144 Hz to 244 Hz with shims removed, and the image results were not significantly affected based on a qualitative assessment of image quality.

Table 1 compares the 3 reconstruction strategies along with prospectively gated acquisition, in terms of ghosting artifact intensity and the signal/noise ratio, using data

from a single mouse. Ghosting artifact was measured by a region-of-interest (ROI) intensity magnitude in the air background in the phase encoding direction, relative to an ROI signal intensity in the ventricles. Signal/noise ratio was measured from the ROI signal intensity in the ventricles relative to the SD in the air background in the frequency encoding direction. The ghosting levels in the retrospectively gated data showed that averaging was more effective than sorting in reducing motion artifact. The prospectively gated images had somewhat better ghosting ratios than the sorted retrospective images, as expected. Meanwhile, the signal/noise ratio for each reconstruction case scaled in accordance with the amount of signal averaging performed, as indicated under the “nex” column.

Figure 4 shows results obtained from 3 mice in parallel. The 50 acquired phases were subdivided into 5 sets of 10, each set interpolated to and reconstructed at 10 time points, and then the 5 sets averaged together. Temporal

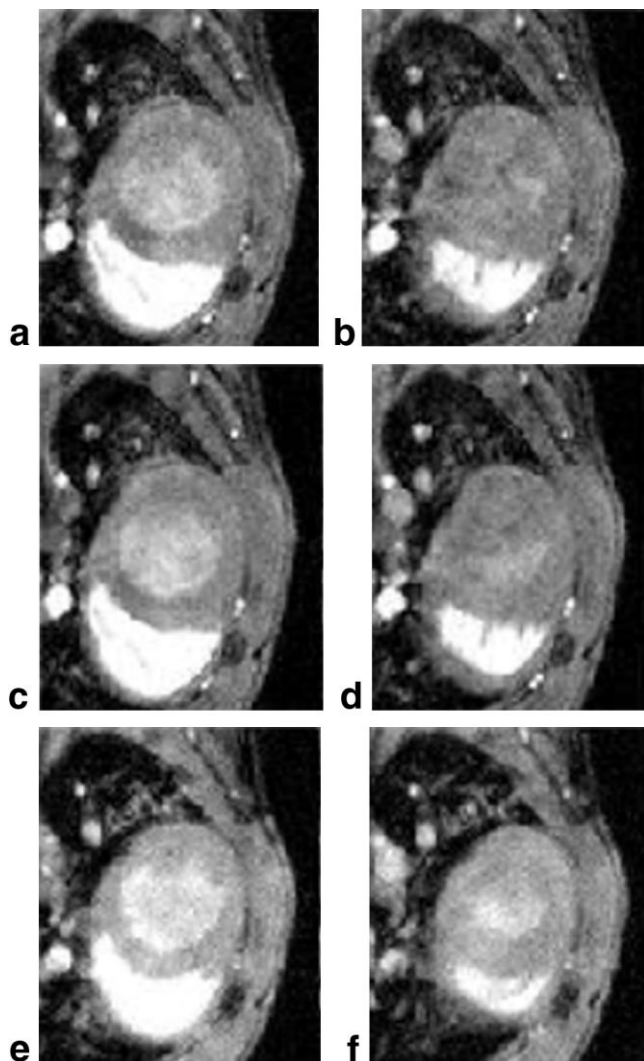


FIG. 3. A mid-axis slice reconstructed at end-diastole (a, c, e) and end-systole (b, d, f) time points. Retrospective reconstruction with sorting (reconstruction strategy 1, a, b) is compared with averaging (reconstruction strategy 3, c, d) and prospective cardiac-respiratory gating (e, f).

Table 1
Comparison of Ghost Artifact in Cardiac Cine Reconstructions

		Ghost/heart ratio (%)	Signal/ noise	nex
Retrospective	1 quiescent sort	11.2	32	3
	2 unsorted	11.9	31	3
	3 averaged	9	41	5
Prospective		9.3	33	3

Phases 1, 4, 7, and 10 of 10 are shown from left to right, of a single slice from each of mice 1–3 (rows 1–3). Row 4 shows mouse 1 at the same slice position as row 1, but imaged separately, by itself, with otherwise identical scan parameters as the data in row 1. The image quality in this figure is somewhat compromised by the poorer temporal sampling of the RR interval and the longer echo time, compared to the images obtained with the small-bore gradient coil. However, a comparison of rows 1 and 4 indicates that similar image quality is achieved in 1 mouse as in 3.

DISCUSSION

From this proof of principle experiment, scaling up to more mice requires only the additional monitoring hardware and receivers, but no additional procedures. A key requirement of multiple mouse imaging with separate receiver coils per mouse is that there be little to no electromagnetic interaction between coils. We have previously measured inter-coil ghosting artifacts and found that the minimum isolation between any pair of coils in our 7 coil array is 47 dB (data not shown). A second possible difficulty may be encountered in double-oblique volume prescription. If there is significant variation in the long axes of the hearts of the mice, it will not be possible to prescribe slabs having independent double-oblique angles per mouse with the common gradient coil. However, if isotropic voxel dimensions are prescribed, a transverse slab orientation could be reformatted into the desired long or short axis views at post processing, with considerable savings in prescan time. Transverse slabs would also preclude the task of optimizing gradient waveforms for minimum echo-time in double-oblique scanning (19). In the present single mouse experiments in the small-bore gradient coil, 255 μm isotropic voxels could have been prescribed for equivalent signal/noise ratio in the 30 min of scan time. Assuming that scan time may be extended to as much as 3 hours in an anesthetized mouse, that a phased array coil that doubles the signal/noise ratio of the existing volume coils is available, and that a large-bore gradient coil better-optimized for cardiac imaging was available, we could reasonably expect to achieve isotropic voxels of 150 μm in multiple mice.

Three-dimensional acquisition is useful for the signal averaging benefit but reduces inflow contrast (20). Significant void artifacts in the ventricles are present in the scan data. We expect that intravascular blood-pool contrast agents (21,22) will be readily available for animal use to provide significantly brighter blood signal. Alternatively, with an appropriate gradient coil fully balanced steady

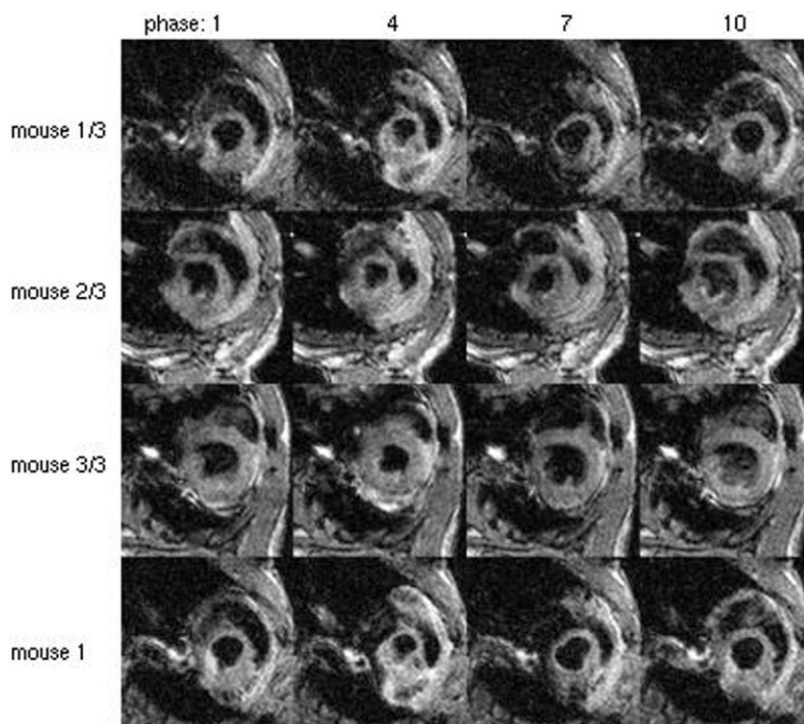


FIG. 4. A mid-axis slice in 3 mice in parallel acquisition, reconstructed at 4 temporal phases throughout cardiac cycle (rows 1–3). The fourth row shows the same slice in mouse 1 as in row 1, but obtained from mouse 1 in single acquisition.

state imaging may be used to achieve better myocardium-blood contrast and better flow tolerance (23).

Averaging for respiratory motion artifacts was surprisingly effective at reducing motion ghosts. This result contrasts with the results of (24), but is in agreement with (3). It is possible that the longer 3-dimensional acquisition introduces additional variability in the k -space trajectory with respect to the cardiac motion such that motion ghosting is less coherent than in 2-dimensional images and is better suited to averaging. Furthermore, we found that anesthetized mice may draw as few as 30 breaths per minute in the latter stages of a long experiment, thus greatly reducing the influence of motion on the data.

Accurate retrospective reconstruction requires high-quality gating signals. Physiologic monitoring hardware is subject to inconsistent placement and contact during preparation of the mice, as well as external signal interference. In this study, we found the ECG monitoring to be highly reliable. The monitoring hardware had effective gradient and RF filters plus optical signal transmission out of the bore of the magnet. In the event that reliable ECG gating cannot be obtained, self-gated ECG methods (25) may potentially be applicable. However, such methods are dependent on the repetition time $TR \ll RR$, which is not easily achieved in a mouse, and on surface coils for signal localization that are not currently available for mouse imaging.

Gradient coil technology is an important part of multiple mouse cardiac imaging. While human clinical imaging systems are capable of sustaining very high rms current necessary for achieving fully balanced gradient echo imaging and high temporal sampling of the RR interval (i.e., $TR \ll RR$), small animal systems may have lower specifications. Our present 29 cm diameter gradient coil can achieve minimum TR/TE of about 50/3.5 ms on a typical cardiac imaging protocol. Ideally, we would like to have a

multiple-mouse cardiac imaging coil of 15 cm diameter, capable of 10–20 G/cm gradient amplitudes at duty cycle of near 100%. In lieu of such a coil, this proof-of-principle experiment shows everything else that is required to perform multiple cardiac mouse imaging. Although our temporal sampling in multiple mice did not meet the objective of $tr \ll RR$, retrospective gating and reconstruction can still be performed if $tr \leq RR$. In this case, scan times are much longer and the temporal sampling of the RR interval becomes somewhat randomized. It has been predicted that the additional ghosting artifact at retrospective reconstruction resulting from randomized temporal sampling is bounded (26).

CONCLUSIONS

It has been shown that retrospective reconstruction provides good image quality, nearly equivalent to prospective acquisition in an equal amount of scan time, on the basis of ghosting intensity. If additional scan time is taken to oversample the respiratory motion, signal averaging is more effective at reducing the motion ghosting than sorting of the respiratory gating data. This may be due to a combination of the non-coherent nature of the motion ghosts that results from the 3-dimensional ky - kz -time sampling trajectory as well as some inconsistencies in the performance of the respiratory monitoring apparatus. It should be noted that excessive averaging will produce blurring in addition to reducing ghost intensity (27), but that has not been analyzed in this study.

Equivalent image quality was obtained with and without slab shimming of the heart, indicating that lack of shimming will not be a significant problem for cardiac multiple mouse MRI. Indeed, the beating heart is very difficult to shim in the first place due to susceptibility (28), motion,

and flow, so for that reason skipping the shim even on a single mouse is not a large sacrifice considering the savings in prescan time.

Preliminary images acquired in 3 mice were similar in quality to an image obtained in 1 mouse. We conclude that combined retrospective cardiac and respiratory gating may be used to perform cardiac imaging of multiple mice, in the context of multiple non-interacting RF coils and a common gradient coil (5).

ACKNOWLEDGMENTS

We thank Dr. S. Berr and Dr. F. Epstein (University of Virginia) for providing the black blood contrast sequence.

REFERENCES

1. Doevendans PA, Daemen MJ, de Muinck ED, Smits JF. Cardiovascular phenotyping in mice. *Card Res* 1998;39:34–49.
2. James JF, Hewett TE, Robbins J. Cardiac physiology in transgenic mice. *Circ Res* 1998;82:407–415.
3. Ruff J, Wiesmann F, Lanz T, Haase A. Magnetic resonance imaging of coronary arteries and heart valves in a living mouse: techniques and preliminary results. *J Magn Reson* 2000;146:290–296.
4. Himes N, Min JY, Lee R, Brown C, Shea J, Huang X, Xiao YF, Morgan JP, Burstein D, Oettgen P. In vivo MRI of embryonic stem cells in a mouse model of myocardial infarction. *Magn Reson Med* 2004;52:1214–1219.
5. Bock NA, Konyer NB, Henkelman RM. Multiple-mouse MRI. *Magn Reson Med* 2003;49:158–167.
6. Dazai J, Bock NA, Nieman BJ, Davidson LM, Henkelman RM, Chen XJ. Multiple mouse biological loading and monitoring system for MRI. *Magn Reson Med* 2004;52:709–715.
7. Bishop JE, Bock N, Nieman BJ, Dazai J, Davidson L, Henkelman RM. Multiple mouse MRI of 16 mice. In: *Proceedings of the 12th Annual Meeting of the ISMRM, Kyoto, Japan, 2004*. p 1753.
8. Beringer WH, Redington RW, Doherty P, Lipton MJ, Carlsson E. Gated cardiac scanning: canine studies. *J Comput Assist Tomogr* 1979;2:155–163.
9. Ritman EL. Micro-computed tomography—current status and developments. *Annu Rev Biomed Eng* 2004;6:185–208.
10. Bohning DE, Carter B, Liu S, Pohost GM. PC-based system for retrospective cardiac and respiratory gating of NMR data. *Magn Reson Med* 1990;16:303–316.
11. Pelc J, Herfkens R, Shimakawa A, Enzmann D. Phase contrast cine magnetic resonance imaging. *Magn Reson Q* 1991;7:229–254.
12. Lenz GW, Haacke EM, White RD. Retrospective cardiac gating: a review of technical aspects and future directions. *Magn Reson Imaging* 1989;7:445–455.
13. Berr SS, Roy RJ, French BA, Yang Z, Gilson W, Kramer CM, Epstein FH. Black blood gradient echo cine magnetic resonance imaging of the mouse heart. *Magn Reson Med* 2005;53:1074–1079.
14. Drangova M, Fredrickson JO, Pelc NJ. An improved method for coronary flow measurement using simultaneous resolution of the cardiac and respiratory cycles. In: *Proceedings of the 5th Annual Meeting of the ISMRM, Vancouver, Canada, 1997*. p 109.
15. Williams SP, Gerber HP, Giodano FJ, Peale FV, Bernstein LJ, Bunting S, Chien SS, Ferrara N, van Bruggen N. Dobutamine stress cine-MRI of cardiac function in the hearts of adult cardiomyocyte-specific VEGF knockout mice. *J Magn Reson Imag* 2001;14:374–382.
16. Streif JUG, Herold V, Szimtenings M, Lanz TE, Nahrendorf M, Wiesmann F, Rommel E, Haase A. In vivo time-resolved quantitative motion mapping of the murine myocardium with phase contrast MRI. *Magn Reson Med* 2003;49:315–321.
17. Epstein FH, Yang Z, Gilson WD, Berr SS, Kramer CM, French BA. MR tagging early after myocardial infarction in mice demonstrates contractile dysfunction in adjacent and remote regions. *Magn Reson Med* 2002;48:399–403.
18. Earls JP, Ho VB, Foo TK, Castillo E, Flamm SD. Cardiac MRI: recent progress and continued challenges. *J Magn Reson Imag* 2002;16:111–127.
19. Bernstein MA, Licato PE. Angle-independent utilization of gradient hardware for oblique MR imaging. *JMRI* 1994;4:105–108.
20. Alley MA, Napel S, Amano Y, Paik DS, Shifrin RY, Shimakawa A, Pelc NJ, Herfkens RJ. Fast 3D cardiac cine imaging. *J Magn Reson Imag* 1999;9:751–755.
21. Amano Y, Herfkens RJ, Shifrin RY, Alley MT, Pelc NJ. Three-dimensional cardiac cine magnetic resonance imaging with an ultrasmall superparamagnetic iron oxide blood pool agent (NC100150). *J Magn Reson Imag* 2000;11:81–86.
22. Hofman MB, Henson RE, Kovacs SJ. Blood pool agent strongly improves 3D magnetic resonance coronary angiography using an inversion pre-pulse. *Magn Reson Med* 1999;41:360–367.
23. Jung BA, Henning J, Scheffler K. Single-breathhold 3D-trueFISP cine cardiac imaging. *Magn Reson Med* 2002;48:921–925.
24. Cassidy PJ, Schneider JE, Grieve SM, Lygate C, Neubauer S, Clarke K. Assessment of motion gating strategies for mouse magnetic resonance at high magnetic fields. *J Magn Reson Imag* 2004;19:229–237.
25. Larson AC, White RD, Laub G, McVeigh ER, Li D, Simonetti OP. Self-gated cardiac cine MRI. *Magn Reson Med* 2004;51:93–102.
26. Roerdink JBTM, Zwaan M. Cardiac magnetic resonance imaging by retrospective gating. *Euro J Appl Math* 1993;4:241–270.
27. Wang Y, Grist TM, Korosec FR, Christy PS, Alley MT, Polzin JA, Mistretta CA. Respiratory blur in 3D coronary MR imaging. *Magn Reson Med* 1995;33:541–548.
28. Atalay MK, Poncetlet BP, Kantor HL, Brady TJ, Weisskoff RM. Cardiac susceptibility artifacts arising from the heart-lung interface. *Magn Reson Med* 2001;45:341–345.